Onset of superconductivity in ultrathin granular metal films

H. M. Jaeger,* D. B. Haviland, B. G. Orr,† and A. M. Goldman
School of Physics and Astronomy, University of Minnesota, Minneapolis, Minnesota 55455
(Received 13 October 1988)

The evolution of superconductivity in ultrathin films of Sn, Pb, Ga, Al, and In has been examined as a function of thickness and temperature. The films were grown in increments by condensation from the vapor onto substrates held at temperatures below 18 K. For each metal, global superconductivity or zero electrical resistance was found when the normal-state sheet resistance R_N fell below a value close to $h/4e^2$, or 6.45 kΩ/□, an observation uncorrelated with either structural or material parameters such as thickness or transition temperature. Prior evidence of superconductivity with nonzero resistance, local superconductivity, was found at earlier stages of film growth. All evidences of superconducting behavior were observed at temperatures close to the bulk transition temperature beginning in the range of thicknesses for which normal-state resistivities were greater than 200 μΩ-cm and were rapidly changing with thickness. This implies that the films consisted of fully superconducting grains connected by tunneling junctions. The strong disorder represented by a broad distribution of junction parameters can be renormalized into weak disorder. Thus theoretical calculations based on regular arrays of superconducting sites coupled by (Josephson) junctions appear to be relevant. The extreme thinness of the films implies very small junction capacitances leading to large quantum fluctuations of the phase differences of their superconducting order parameters. Two classes of theories explaining a nearly universal resistance threshold for superconductivity have emerged. Both classes involve the quenching of these quantum fluctuations. In the limit of very small junction capacitances the threshold occurs at resistance values near $h/4e^2$, and is essentially independent of the capacitance and the energy gap, in good agreement with the experimental data. Not contained in any of the models is an explanation of the observed regular variation of the low-temperature resistances of the films with the normal-state sheet resistance for values just above the resistance threshold.

I. INTRODUCTION

Ultrathin films prepared by deposition onto substrates held at temperatures near those of liquid helium have been studied since the pioneering work of Shal'nikov[1] and Buckel and Hilsch.[2] Early research in this area was directed at studying the properties of amorphous metals which often result when substrates are kept cold. The promise of substantially elevated superconducting transition temperatures which was implied by some of the early results was never realized in practice. Nevertheless detailed investigations of the electron-phonon coupling in amorphous thin films were carried out through tunneling experiments, yielding an understanding of the elevation of T_c of amorphous superconductors relative to bulk crystalline metals.[3] Quench-evaporated films played a major role in the development of the understanding of superconducting fluctuations,[4] in the study of localization,[5] and in the interplay between localization effects and superconductivity.[6]

In most studies of quench-evaporated films the vapor sources have been filaments, open boats, or electron guns. The vacuum environments were pumped in a conventional manner, but with substantial assistance from the cryopumping action of surfaces cooled to liquid-helium temperatures. In a recent series of investigations,[7–10] a different approach to the deposition of films onto low-temperature substrates was developed.[11] This involved the use of commercial Knudsen cells as vapor sources in an UHV environment pumped using ion pumps, and resulted in films with thicknesses of nominal uniformity as determined by geometry of better than one part in 10^4. The techniques employed substantially mitigated the problem of outgassing from the walls which contaminates films prepared in environments in which most of the pumping is cryopumping. The particular apparatus which was developed also permitted the study of the thickness dependence of the electrical properties of films as the vacuum environment was sufficiently clean that material could be deposited on the substrate in small increments with extensive electrical and magnetic studies being performed between successive depositions. With this approach, transition temperature oscillations with thickness were observed in ultrathin films,[7] and a series of investigations were undertaken which revealed the nature of the onset of superconductivity in ultrathin films as they were grown on a bare substrate.[8–10] The latter work will be discussed here.

An important feature of the early stages of the growth of superconducting films is that the general behavior of $R(T)$ with thickness resulting from the above approach is surprisingly reproducible. This is true for a variety of soft metals such as Al, Ga, In, Pb, and Sn. The thinnest films are disconnected and no current flow can be measured. When films become connected, the curves of $R(T)$ exhibit strong negative temperature coefficients of resistance (TCR) which can be attributed to conduction by electron hopping between metal clusters. As film

thicknesses are increased further, a sharp change in the slope of $R(T)$ can be observed at temperatures close to the T_c of the corresponding bulk material. This is followed by the development of a local minimum in $R(T)$ which deepens and eventually flattens out as the thickness is increased further. Subsequent addition of material then leads to globally superconducting behavior (zero resistance). Most remarkably, the latter is correlated with the normal-state sheet resistance of a film falling below a threshold value very close to $h/4e^2$ or 6.45 $k\Omega/\square$ and furthermore is independent of material and film thickness.

The focus of this paper will be in describing the experiments and the nature of the films so as to provide a framework for understanding the two classes of models which have been presented to explain the onset of global superconductivity. In the first class of models, which employs the ideas of Caldeira and Leggett,[12] the threshold follows from the suppression of zero-point quantum phase fluctuations by dissipation in Ohmic conduction channels which are in parallel with the Josephson tunneling channel. In the second class, the virtual tunneling of quasiparticle excitations results in a renormalization of the capacitances of the junctions, bringing about the suppression of the fluctuations and the onset of superconductivity.[13] Both classes predict a nearly universal threshold in the regime of large charging energies $E_c = e^2/2C$ and thus may apply in the circumstance of very thin films which can be modeled as Josephson coupled superconducting clusters with very small capacitances. The role of the normal channels (either Ohmic shunt or quasiparticle) is the unique feature which changes the threshold for superconductivity in such systems from the well-known nonuniversal Anderson-Abeles[14] form to a nearly universal one. The Anderson-Abeles approach to the superconducting threshold ignores dissipation and only considers the relative strengths of the Josephson coupling and charging energies, the latter being associated with the zero-point fluctuations of the phase of the superconducting order parameter.

In Sec. II we will present the features of the experimental configuration which we believe uniquely permit measurements of the type reported in Sec. III. Section IV will contain a simplified treatment of the theoretical models and their applicability to disordered films, and Sec. V will contain a discussion of the agreement of experiment and theory. The final section will summarize the work and address outstanding questions.

II. EXPERIMENT

The apparatus used differs from that first developed by Shal'nikov[1] and later by Buckel and Hilsch[2] for quench evaporation of metals. The design, which has been described elsewhere,[11] unites the technologies of molecular-beam epitaxy (MBE) and low-temperature cryogenics. A low-temperature apparatus equipped with ^{3}He refrigerator was built onto the top of a MBE growth and analysis chamber. The cold sample platform could be lowered into a growth chamber where the substrate could be subjected to precisely controlled exposures of metal vapor flux. The platform could then be retracted from the growth chamber for *in situ* low-temperature studies of the resultant films.

The metal vapor sources used were commercial Knudsen cells (K cells). These sources employ a deep well (approximately 13.8 cm deep with a 1.8-cm-diam opening) "top hat" pyrolitic boron nitride (PBN) crucible which served to collimate the metal vapor beam. Although not true effusion cells, these sources exhibit substantially less flux divergence than an ordinary shallow crucible, tungsten boat, wire, or basket evaporation sources, which are Langmuir sources. The K cells were heat shielded to prevent outgassing of the growth chamber walls and were operated at a constant temperature. The vapor flux was controlled by cooled tantalum shutters positioned in front of each cell. This made possible the deposition of increments of average film thickness of less than 0.02 Å. The source-to-substrate distance was approximately 45 cm and the film dimensions, defined by a mask, were 5.0 mm by 0.5 mm. With these geometrical factors and the standard $\cos\theta$ law for film thicknesses, the gradient in average thickness was estimated to be much less than 1 part in 10^4 across the length and width of the film.

A calibrated crystal oscillator thickness monitor was used to measure the amount of material deposited during each exposure of the substrate. The stated thicknesses of films are nominal in that they are determined from summing the mass increments of material deposited on the thickness monitor during each deposition and using the standard bulk density. The latter may not be the actual density of material deposited onto a cold substrate. The monitor was calibrated by depositing a Sn film at ambient temperature and measuring its thickness using a profilometer. All films were grown on silica-glazed alumina substrates which were 2.54 cm square and 0.625 mm thick. The glaze was 0.013 cm in thickness and provided a very smooth surface on atomic length scales with variations occurring only at long wavelengths.

The substrate was affixed to a large copper block whose temperature was monitored using a Ge resistance thermometer. By thermal coupling of this block to a pumped ^{4}He reservoir and by liquid-nitrogen heat shielding of the part of the cryostat insert that was lowered into the growth chamber, the substrate temperature could be held between 15 and 18 K during metal deposition. This is a somewhat higher temperature than used by other workers[2,15,16] and may have resulted in less contamination of the films by gases adsorbed and trapped during deposition. The pressure in the growth chamber was less than 2×10^{-10} torr during evaporations, with the dominant residual gas being H_2. The degree of control of film thickness offered by this apparatus allowed the study of the evolution of a *single film* through all stages of its electrical transport behavior.

Measurements of electrical transport properties were carried out *in situ* as the thickness of a single film was incremented through successive depositions of metal. Four-terminal measurements were accomplished by using several stages of connection to the film. Moving from the electrical wires towards the film each state of connection became progressively thinner. Wire leads were soldered

onto 5000-Å-thick silver pads which had been evaporated onto the substrate before loading it into the UHV system. These pads made contact with 100-Å-thick leads which were deposited after loading into the UHV system. A mask blocking the portion of the patterned area constituting the film was then removed and the film growth was begun. The film structure itself was ten squares long. Four tabs which were a part of the evaporated strip made contact with the thicker leads.

After each increment of metal was deposited, the cryostat was retracted into the low-temperature environment. A pumped ^{3}He pot was used to cool the sample to 0.7 K (0.6 K in the case of Al films). The temperature was mainly limited by both a strong thermal connection of the sample holder to the 1-K pot, and limitations of the pumping speed in the flexible connection between the cryostat and the vacuum pump.

Resistance measurements were made using either an ac or dc four-terminal configuration, or a four-terminal ac bridge arrangement. The electrical leads to the cryostat were provided with rf filters, and the environment of the cryostat was magnetically shielded with a μ metal can. Most measurements were controlled by an Apple II+ personal computer which communicated with the instruments through an IEEE-488 interface. Temperature was measured and controlled by a Quantum Design Digital R/G Bridge. Four-terminal dc measurements were made using a Keithley Model 220 Current Source and a Keithley model 181 Nanovoltmeter with careful filtering of radio frequency interference. In some instances a PAR 113 amplifier was employed. All ac measurements were carried out using an EG&G/PAR 5206 two-phase lock-in amplifier. In the case of the measurements on Al films, dc four-terminal measurements were not computer controlled. For this work a battery-powered current source was employed together with a battery-operated Keithley Model 148 Nanovoltmeter.

Measurements in a magnetic field were limited to the perpendicular direction and to fields of 2 kOe. This was a consequence of the geometry of the apparatus. The plane of the film was along the axis of the cryostat, necessitating the use of a transverse split coil with a limited field range.

III. EXPERIMENTAL RESULTS

The apparatus described in the preceding section permitted the study of the dependences of resistance on thickness, temperature, and magnetic field. The thickness dependence of the normal-state resistance will be considered first as it gives important clues as to the structure of the films which cannot be determined directly.

Figure 1 shows the sheet resistance of the normal state R_N as a function of the nominal film thickness d for several of the different metals studied. R_N is represented by the resistance at 14 K, i.e., $R_N = R$ (14.0 K). This choice is purely operational and was motivated by the fact that at 14 K the film is safely above the bulk transition temperature, T_{c0}, of the materials used and most of the temperature dependence of $R(T)$ has ceased. Also up to this temperature annealing effects are still safely

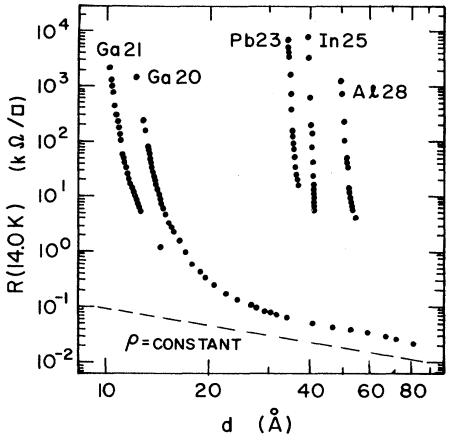

FIG. 1. A log-log plot of the normal-state resistance R(14.0 K) vs the nominal thickness d for Ga, Pb, In, and Al. R(14.0 K) is a rapidly decreasing function of thickness in the region of film growth where superconductivity emerges. In the case of the film labeled Ga20, film growth was taken to larger thicknesses where the resistivity ρ approached a constant value.

avoided. Common to all five curves in the figure is an extreme sensitivity of the normal-state resistance to thickness changes in the early stages of film growth. Adding only a small amount of material after the first measurable onset of electrical conduction results in R_N dropping by several orders of magnitude. For the sequence of gallium films shown in Fig. 1 we followed the behavior out to higher d, observing a crossover to much weaker dependence of R_N on d, but up to 80 Å the resistivity $\rho = R_N d$ was not completely independent of d as would be expected in the bulk limit. The data clearly show that the average thickness for initial connectedness varied for different materials, and also for different films of the same material due to variations in the local topology and wetting characteristics.

Figures 2(a)–2(d) show the evolution with thickness of $R(T)$ curves of aluminum, indium, lead, and gallium films as the amount of material deposited was increased in very fine successive steps. Typically increments between 0.05 and 0.2 Å were used in the evaporations once initial electrical connectivity across a sample was established. In general the evolution can be characterized by three major stages: nonsuperconducting, locally superconducting, and globally superconducting. These stages were found in all films reported here as well as in previous work on Sn films.[8,9]

The thinnest films exhibit strong insulating behavior and activated conductivity with no trace of superconductivity. Manifestations of superconducting order (local superconductivity) first become noticeable for slightly thicker films in the form of a kink and eventually a dip (local minimum) in $R(T)$. The latter behavior has been called "quasireentrant" superconductivity because the resistance never actually drops to zero.

The local transition temperature $T_c^{\rm loc}$, defined by

$R(T_c^{loc}) \equiv \frac{1}{2}R_N$, is presumably related to the onset of superconducting order in the grains or clusters which constitute the film. This superconducting order in the entire film can be neither long range nor quasi-long range as the electrical resistance does not fall to zero. Figure 3 shows the behavior of T_c^{loc} as a function of sheet resistance R_N.

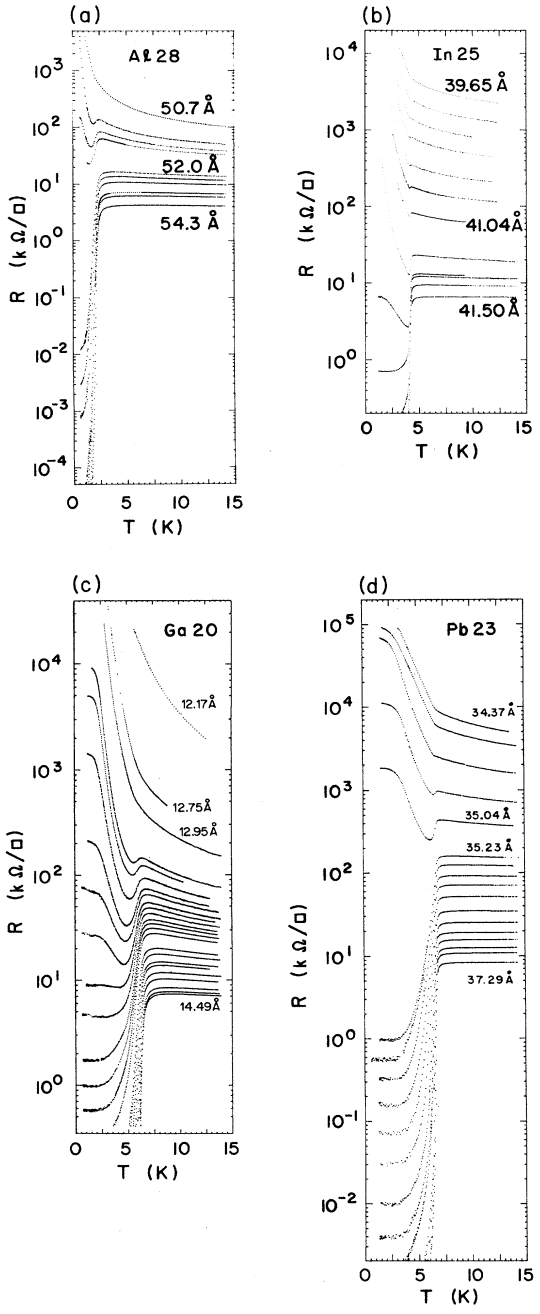

FIG. 2. The evolution of $R(T)$ curves for (a) Al, (b) In, (c) Ga, and (d) Pb, obtained *in situ* after successive increments of film thickness. Note that in all cases the entire evolution from insulating to globally superconducting spans an interval of nominal thickness of less than one monolayer.

In Pb and In films there was no significant change in the transition temperature with sheet resistance over the several decades in R_N. For Al and In films T_c^{loc} was enhanced relative to the bulk transition temperatures 3.7 and 1.2 K, respectively. For Ga films the transition temperature was reduced in a manner proportional to $\log_{10}(R_N)$ over several decades in R_N. The Ga films were about a factor 3 thinner than the Al, Pb, and In films of the same R_N. Thicker Ga films, with consequently lower R_N, showed no significant reduction in T_c^{loc} and their transition temperatures with increasing thicknesses converged to the reported[17] value of 8.4 K for thick films of quench-evaporated Ga. Behavior similar to that found in Al and In films was also observed for Sn films prepared in the same apparatus.[8] However, some of the thicker Sn films also exhibited transition temperature oscillations with thickness.[7]

It should be pointed out that the above definition of the local transition temperature is an operational one and particularly in very thin films the resistive transitions are fairly broad. Because the major broadening of the resistive transitions of the films is found for values of $R(T)$ well below $0.5R_N$, the half point is probably still a good definition of the local transition temperature.

As the thickness is increased further, the "quasireentrant" behavior gives way to zero resistance or global superconductivity. There is a transition region between the "quasireentrant" and globally superconducting regions in which $R(T)$ drops several decades as the temperature is lowered but eventually flattens off and appears temperature independent down to the lowest temperatures measured (~ 0.60 K). As more metal is deposited, the residual low-temperature resistance of these "flat tails" very rapidly drops below the limit of experimental resolution. The latter is determined both by the signal-to-noise ratio of the lock-in amplifier and by the maximum measuring current that does not produce either heating or nonlinear

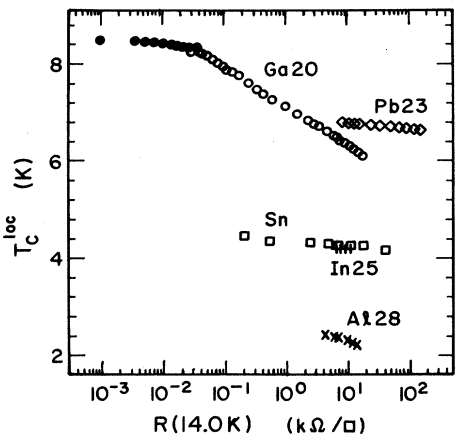

FIG. 3. The local transition temperature T_c^{loc} as a function of the normal-state resistance $R(14.0\text{ K})$, for Ga, Pb, Sn, In, and Al. T_c^{loc} is defined by $R(T_c^{loc}) = \frac{1}{2}R(14.0\text{ K})$. The solid circles are data on thicker Ga films taken from Ref. 17.

effects. For our experiments this resistance was of order 1 mΩ.

It is very important to keep in mind that the whole evolution described above for all systems studied took place over nominal thickness intervals corresponding to *less than one atomic layer.* The total average thickness at which this evolution would take place on the other hand was found to vary from sequence to sequence, even for the same material [see the thickness values indicated in Figs. 2(a)–2(d)]. It is also evident that the transitions between the first two stages of the evolution do not correspond to particular values of the sheet resistance. Nevertheless, the data can be used to show that the transition to the third stage, global superconductivity, is dependent on a particular critical value of the sheet resistance in the normal state R_N. The evidence for this comes from an analysis of the dependence of low-temperature resistance in the flat-tail regions on R_N.

It should be noted that the flattening off of the rising resistance at the lowest temperatures of the quasireentrant traces in Figs. 2(a)–2(d) may arise from effects very different from those responsible for the previously discussed flat-tail region. First, the low-temperature resistance of very highly resistive quasireentrant films approaches values where the leakage resistance to ground of the electrical wiring is no longer negligible. Second, when observed, the flattening off proved to be current dependent even at the low measuring currents of ~1 nA used when measuring the quasireentrant stage of the evolution. Examination of the *I-V* characteristics in those cases showed that the currents were large enough to bias the sample into regimes of significant nonlinearity. Since the nonlinearity of the *I-V* characteristics moves to lower currents with decreasing temperature, a flattening off of the $R(T)$ curves results. In the flat-tail region, on the other hand, no current dependence was observed unless the sample current significantly exceeded the values of 0.5–5 μA used which were chosen to stay within the linear portion of the *I-V* characteristics.

Typical *I-V* characteristics corresponding to the individual traces in the $R(T)$ evolution are shown in Fig. 4 for one Ga sequence. Evident is a gradual transition from what might be termed "quasi-particle-like" to "Josephson-like" behavior. "Quasi-particle-like" *I-V* characteristics exhibit a nonlinear upturn in current once a certain voltage level is reached and "Josephson-like" characteristics exhibit a nonlinear upturn in voltage beyond a certain current level. The thinnest films in a sequence, which display local superconductivity with a kink or dip in $R(T)$, have "quasi-particle-like" characteristics. For single junctions such a feature is the signature of the gap in the excitation spectrum and at higher voltages the characteristic would be Ohmic. Because the films were thermally unstable at the high currents required to enter the Ohmic regime, it was necessary to truncate the *I-V* characteristic at voltages just above those corresponding to the nonlinear upturn in current.

As more material is deposited the "gap" feature becomes less and less pronounced and finally vanishes completely (see Fig. 4, trace *f*). Films for which this happens also exhibit flat tails in $R(T)$. This correspondence between the changes in the *I-V* characteristics and $R(T)$ has been found in all sets of films which have been prepared.

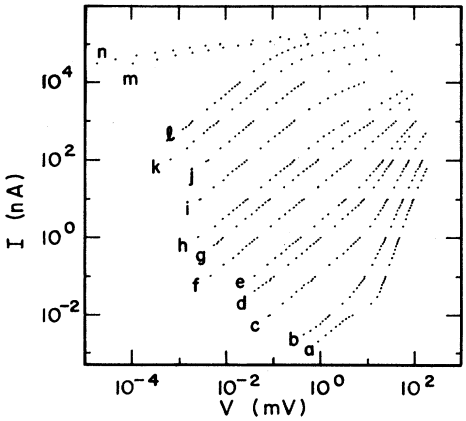

FIG. 4. *I-V* characteristics taken at $T=0.7$ K for the Ga20 sequence. The thicknesses from trace *a* to trace *n* span the range 13.09 to 14.54 Å. Traces *a* through *e* correspond to "quasireentrant" $R(T)$ curves in Fig. 2(c). Traces *f* through *l* correspond to $R(T)$ curves exhibiting flat tails. The transition to global superconductivity occurs between traces *l* and *m*.

An important common feature of the *I-V* characteristics measured at 0.7 K was a linear regime at low currents. Only at higher currents did nonlinearities set in. Figure 5(a) shows in greater detail the *I-V* characteristics of four films of the aluminum sequence close to the threshold for global superconductivity. The films increase in thickness going from traces *A* to *D*. As the normal-state resistance of a film decreases with increasing thickness, the corresponding low-temperature *I-V* characteristics, as in Fig. 4, suddenly become strongly nonlinear over the entire measured current range. This transition coincides with the onset of global superconductivity. Figure 5(b) shows the corresponding $R(T)$ traces at temperatures above $T_c^{\rm loc}$. The onset of zero low-temperature resistance occurs as R_N falls below $h/4e^2$, i.e., between traces *C* and *D*.

It is obvious from the figure that a precise definition of any dependence on R_N is limited by the existence of a small, but significant negative TCR even up to 14 K. Such a negative TCR was also present in other materials investigated, with the exception of Pb.

Figure 6 shows that the transition to "global superconductivity," or nominal zero resistance at low temperature, is independent of average film thickness. Included in the figure are results on Ga, Sn, Al, and Pb films. The pairs of data points connected by vertical lines correspond to the normal-state sheet resistances of two particular traces belonging to sequences of films of the kind shown in Figs. 2(a)–2(d). The upper point (open symbol) identifies the value of R_N of the last trace in a sequence for which the resistance did not vanish at low temperatures. The lower point (solid symbol) corresponds to the R_N of the subsequent, globally superconducting trace in the same sequence. The thickness increments between

successive traces in most cases were so small (fractions of an Angstrom) that the connecting lines appear vertical in the figure. Over the whole thickness range from 12–52 Å a resistance value of 6.45 kΩ/□ is always bracketed by the pairs of points in the figure. The spread in the resistance values of the pairs is due to the extreme sensitivity of film resistance to even the smallest change in thickness at this stage of film evolution. Figure 6 shows that the films' average thickness d within the critical interval varies substantially both for different films of the same metal and films of different metals. In spite of this variation the data suggest the value $h/4e^2$ as a resistance threshold for global superconductivity independent of both thickness and material.

It should be mentioned that several attempts to grow In films in our system were not successful as far as the determination of the threshold value for zero resistance was concerned because of problems with highly resistive four-point-probe leads. This might have been caused by a particular wetting problem of In on the substrates used. However, this caused no major problem for measurements in the earlier stages of film evolution where the films as a whole were highly resistive [see Fig. 2(b)].

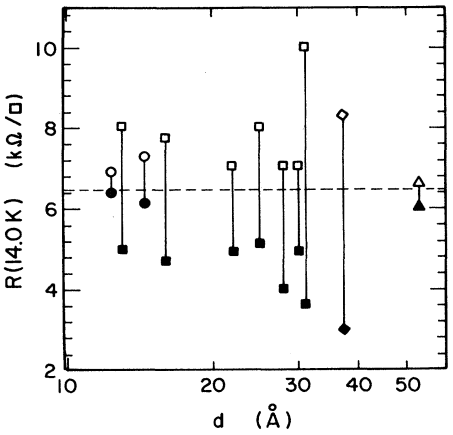

FIG. 6. The pairs of connected points represent the normal-state resistance of successive depositions in sequences of Ga (○), Sn (□), Pb (◇), and Al (△) films. The nominal thickness difference between the connected points is a fraction of an Angstrom and not noticeable on this scale. The upper point (open symbol) of any pair shows the normal-state resistance of the last film in which a resistance at low temperatures could be measured. The lower point (solid symbol) represents the first film where no resistance at low temperatures was found. Independent of material studied or thickness of the film, each pair brackets the normal-state resistance value $R(14.0\ \mathrm{K})=h/4e^2$ denoted by the dashed line.

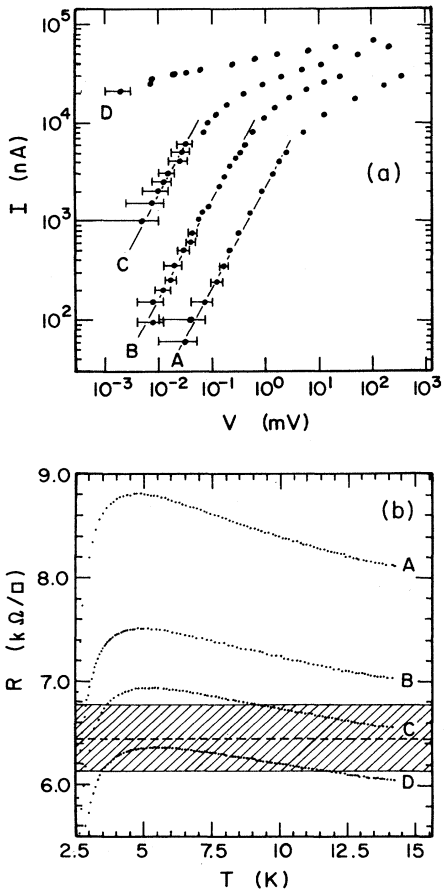

FIG. 5. (a) The I-V characteristics taken at $T=0.6$ K at four stages of the Al28 sequence. (b) The corresponding $R(T)$ traces above T_c^{loc}. Note that between traces C and D, when R_N crosses $h/4e^2$, the low-temperature I-V characteristics no longer show an Ohmic portion. This Ohmic dependence of traces A, B, and C is denoted by the straight lines of slope 1 in (a). The shaded area of (b) shows the resistance interval $h/4e^2\pm5\%$.

The detailed data on Ga, Al, and Pb allow an alternative method for characterizing the approach to zero resistance and identifying the threshold. In Fig. 7 the low-temperature resistance (of the flat tails at $T=0.7$ K) is plotted as a function of the normal-state resistance R ($T=14.0$ K). The low-temperature resistance exhibits a rapid fall by several orders of magnitude as $R_N\rightarrow h/4e^2=R_q$.

If the normal-state resistance controls the transition to superconductivity, then the functional form of the data of Fig. 7 could be used to test theories of such a resistance-controlled transition. Models of the superconducting transition in which resistance plays an important role, which will be discussed in Sec. IV, predict threshold values close to R_q. However, no model contains detailed predictions for the variation of the low-temperature resistance with the normal resistance.

Although a systematic study of the magnetic field dependence of the resistance at every stage of the films' evolution has not been carried out, preliminary results in perpendicular fields have been obtained. These can be summarized in the following way: well above the superconducting transition temperature and for films with $R_N\gtrsim 1$ kΩ/□ there was no significant magnetoresistance.

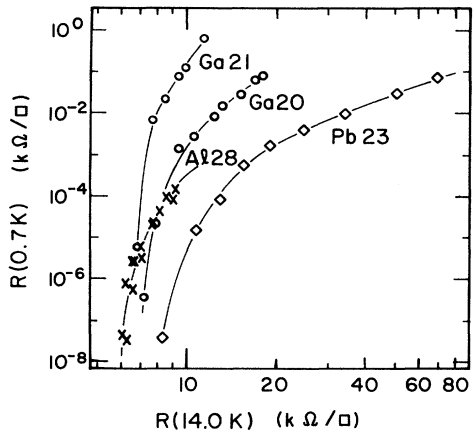

FIG. 7. The resistance of the film at $T=0.7$ K is plotted vs the resistance at $T=14.0$ K [cf. Figs. 2(a)–2(d) and Fig. 8]. As more material is deposited onto the film and the normal-state resistance $R(14.0\text{ K})\rightarrow h/4e^2$, $R(0.7\text{ K})$ rapidly drops several orders of magnitude. The curves are guides to the eye and do not represent a fit to the data, however a theory where the normal-state resistance controls the transition to superconductivity should explain their shape.

Measurements put an upper limit on $\Delta R(H_{\max})/R(0)$ of 0.1%, where $H_{\max}$ was limited to ~ 2 kG. At temperatures below T_c^{loc} the magnetoresistance was always positive up to the maximum measuring field $H_{\max}$. The magnitude of stray fields inside the μ metal shielded cryostat was estimated to be less than 0.01 G. In films with flat tails, which were not globally superconducting (Fig. 8), the resistance increased by a factor of the order of 4 at 100 G.

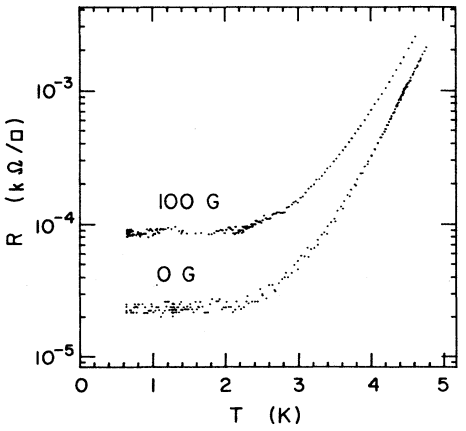

FIG. 8. The effect of a magnetic field on the $R(T)$ trace is shown for a Ga film. A magnetic field of 100 G raised the flat-tail resistance by a factor of 4. For all films, near the threshold to global superconductivity, no magnetoresistance in the normal state was observed at fields up to 2 kG.

IV. MODELS FOR THE ONSET OF SUPERCONDUCTIVITY

In this section we will discuss various theoretical models which have a bearing on the threshold for global superconductivity. The issues associated with the onset and existence of superconductivity in disordered low-dimensional systems have been studied extensively. In attempting to understand these matters it is essential to note that the order parameter for the superconducting state is characterized by both a magnitude and a phase and that either or both of these quantities can play a role in the onset of superconductivity.

The suppression of the superconducting pairing mechanism will result in a depression of the magnitude of the order parameter. Disorder-induced electronic localization can enhance Coulomb repulsion and consequently inhibit or weaken pairing. Within the framework of weak localization theory the consequences of such a microscopic approach have been explored in detail theoretically[18] as well as experimentally in thin films.[16,19] The theories generally predict that $\delta T_c \equiv T_c - T_{c0}$ is linear in $1/d$ for small δT_c, and eventually superconductivity is destroyed as T_c drops continuously to zero from the bulk value T_{c0}. Rather than predicting a universal resistance threshold for superconductivity independent of thickness or material, all models with the above features lead to a smooth, continuous decrease of T_c.

It is necessary to look at the phase of the order parameter and to the conditions associated with the existence of the macroscopic manifestations of superconductivity such as long-range phase coherence and associated zero electrical resistance in order to understand the possible origin of a resistance threshold. In granular systems such as these ultrathin films phase locking occurs by the coupling of the phases of the order parameters between adjacent grains. These matters, rather than microscopic aspects of the pairing mechanism are the focus of our discussion of theory. Before doing this we will examine the conditions for superconducting pairing in the grains themselves. This is important to set the stage for lattice models of the onset of global superconductivity which involve intergrain coupling.

A. Isolated grains

Isolated grains or islands are important at the early stages of film growth. If microscopic disorder within islands is assumed to be negligible, then the determining factor will be their characteristic size L. Neglecting band-structure effects, a grain of size L will exhibit a single-electron energy level spacing $\delta E = 1/N(0) = 1/n(0)L^3$. Here $N(0)$ is the single-electron density of states at the Fermi level and $n(0)$ is the density of states per unit volume. If the level spacing is compared with the magnitude of the superconducting condensation energy, we find that the formation of a superconducting state is favored as long as $\delta E < \Delta$ where Δ is the gap parameter at $T=0$. The above criterion translates into a lower bound for the grain size L which will permit superconducting ordering and is usually written as[20,21]

$$L_{\rm crit} \simeq [n(0)kT_c]^{-1/3} . \quad (1)$$

For typical metals in a free-electron approximation $k_F \simeq 2/\text{Å}$ and $T_c \simeq 1$ K and $L_{\rm crit} \simeq 30$ Å. Thus no superconductivity is expected in grains with $L < L_{\rm crit}$. In fact, a calculation by Strongin *et al.*[22] shows an exponential decrease of T_c as $\delta E/\Delta \sim (L_{\rm crit}/L)^3 \rightarrow 1$. Alternatively Eq. (1) can be interpreted as criterion for the minimum number $N_{\rm crit}$ of electrons necessary on a grain to form a condensate.[23] This number is of order 10^3 for typical metals.

For grains of size L less than the superconducting coherence length ξ_0, Mühlschlegel *et al.*[24] showed that fluctuations of the magnitude of the order parameter lead to significant deviations from Δ, even for values $\delta E/\Delta \ll 1$. Thus in completely isolated grains $L_{\rm crit}$ is presumably even larger than 30 Å.

B. Phase coupling

The establishment of zero-resistance transport between grains or islands will occur when there is a phase coupling of their separate macroscopic wave functions. The energy associated with this is the Josephson coupling energy $E_J(\theta) \equiv E_J(1-\cos\theta)$. Other relevant energies are the thermal energy kT, and the charging energy $E_C \equiv e^2/2C$. In addition, it will turn out that dissipative effects must be included in the model in order to have a resistance threshold. In the following we assume that island or cluster sizes have grown large enough to neglect any level spacing ΔE, and that a superconducting order parameter is established on either side of a junction.

The standard expression for E_J follows from the tunneling Hamiltonian for an ideal superconductor-insulator-superconductor (SIS) junction and is given by[25]

$$E_J = \tfrac{1}{2}\pi^2 \langle |T|^2 \rangle N^2(0)\Delta(T)\tanh[\Delta(T)/2kT] . \quad (2)$$

Here $\langle |T|^2 \rangle$ is the average of the absolute square of the tunneling matrix element. From an analysis of the corresponding normal tunnel junction one defines a normal-state intergrain tunneling resistance

$$R_N^{-1} = \pi^2 (R_q)^{-1} \langle |T|^2 \rangle N^2(0) . \quad (3)$$

Without considering the details of the microscopic relaxation processes that lead to any actual dissipation, R_N in this picture is defined as the effective resistance a normal junction would have in the limit $E_C \rightarrow 0$.[13,26] In this limit the normal tunneling resistance is temperature independent.[27] Using the last expression, the Josephson coupling energy (at $T=0$) is given by

$$E_J = \tfrac{1}{2}(R_q/R_N)\Delta . \quad (4)$$

If the Hamiltonian for a single junction contains only the Josephson coupling term and the charging energy can be neglected, as might be justified for structures with large capacitances, the condition for phase coupling becomes[27]

$$E_J > kT . \quad (5)$$

When the capacitance is small the charging energy $E_C = e^2/2C$ can be comparable or even exceed E_J or kT. Then the threshold criterion in a single junction becomes[28]

$$E_J > E_C + kT/2 . \quad (6)$$

At $T=0$ this reduces to the well-known condition for phase coupling due to Anderson and Abeles:[14]

$$E_J > E_C . \quad (7)$$

The junction is then described by the Hamiltonian

$$H = \tfrac{1}{2}[(2e)^2/C]N^{*2} + E_J(1-\cos\theta) , \quad (8)$$

where $Q = 2eN^*$ is the total transferred charge due to pairs. Equation (8) can be interpreted as Hamiltonian of a phase "particle" in the "washboard" potential $E_J(\theta) = E_J(1-\cos\theta)$. Small zero-point fluctuations in the bottom of the well correspond to energies

$$\hbar\omega_J = (8E_C E_J)^{1/2} . \quad (9)$$

The commutator $[N^*,\theta] = i$ implies an uncertainty relation of the form $\delta N^* \delta\theta > \frac{1}{2}$. Large charging energies prohibit strong fluctuations δN^* and thus give rise to large phase fluctuations $\delta\theta$. These fluctuations disrupt phase coherence unless condition Eq. (7) is satisfied.

The Hamiltonian for an array of junctions with large capacitances can be mapped onto the classical X-Y model. In two dimensions the onset of phase coherence is described by the Kosterlitz-Thouless-Berezinskii (KTB) transition[29] that occurs below T_c at a temperature $T_{\rm KT}$. In ultrathin films consisting of metal islands and in certain structures prepared using modern microfabrication techniques large charging energies are realized. In this instance the appropriate picture is the quantum X-Y model as discussed by a number of workers.[30,31] The onset of long-range phase coherence is then found below a critical ratio E_C/E_J of order unity, confirming the Anderson-Abeles condition Eq. (7).

However, neither classical nor quantum X-Y models lead to a universal resistance threshold for phase coherence. In the KTB transition $T_{\rm KT}$ is continuously depressed to zero as R_N increases,[32] and the ratio E_C/E_J involves the junction capacitance as well as the gap parameter and is therefore thickness and material dependent.

All models described above neglect the normal tunneling currents which flow in addition to the supercurrent. These normal currents can play a role in restoring phase coherence even if the Anderson-Abeles condition $E_C/E_J \leq 1$ is violated. Normal currents have been treated either as flow through an Ohmic shunt resistor, or as the tunneling of quasiparticle excitations. These two descriptions of a tunnel junction lead to two distinct explanations of the restoration of phase coherence. The first is based on the work by Caldeira and Leggett (CL),[12] the second on the model by Ambegaokar, Eckern, and Schön (AES).[13,33]

In the CL model dissipation is taken into account by coupling the quantum-mechanical variable of interest [in this case θ in the Hamiltonian Eq. (6)] to a "heat bath" of

an infinite number of linear oscillators of appropriate spectral strength. Usually this strength is chosen such that the resulting action $S[\theta]$ corresponds to a Langevin equation with a linear dissipation term, i.e., Ohmic dissipation. The weakness of this model, namely the phenomenological nature of the degrees of freedom which are the heat bath, is overcome by the AES model which is based on a microscopic tunneling Hamiltonian. Several calculations have been carried out applying the CL and AES formalisms to both single junctions[34–41] and arrays of junctions.[41–47] All calculations find a threshold value of the resistance above which phase coherence is not possible. However, the predicted value of the threshold resistance is not universal in all calculations and may (weakly) depend on other parameters, e.g., the gap and the charging energy. In any array model there is an additional dependence on the number of nearest neighbors.

The equation of motion of the phase "particle" derived from the CL effective action is that of the resistively shunted junction (RSJ) model.[48] It is closely related to the one derivable from the Hamiltonian Eq. (8) using the Josephson relation[27]

$$V=\hbar\dot{\theta}/2e \tag{10}$$

and the fact that $V=Q/C=2eN^*/C$. In both cases the time evolution of θ can be interpreted as the motion of a phase "particle." The heat bath of the CL action, however, provides an additional damping term proportional to $\dot{\theta}/R$. The phase-coherent, superconducting state of a junction corresponds to a phase "particle" localized in one of the potential wells, whereas the resistive, phase-incoherent state corresponds to diffusion of the "particle" by tunneling along the θ direction.

Models based on the CL action exhibit a transition from the localized to the diffusive state depending on the strength of the dissipation. Initial calculations for single junctions at $T=0$ (Ref. 34) have subsequently been extended to finite temperatures[35–39] and D-dimensional arrays of identical junctions.[42–45] In order for phase coherence to exist, the shunt resistance R has to fall below a critical value $R_{\rm crit}$, listed in Table I. In array models of this type, in contrast to single-junction calculations, the threshold at $R_{\rm crit}$ is only universal, i.e., independent of E_C or Δ, in the limit of strong charging $E_C/E_J \gg 1$. For smaller E_C the threshold depends weakly (logarithmically) on E_C and eventually reduces to the Abeles-Anderson result, i.e., Eq. (7).

The correct interpretation of R as either the low-voltage (subgap) quasiparticle (QP) resistance, $R_{\rm QP}$, or the normal-state resistance is still an open question. Fits to predicted escape rates measured in macroscopic tunneling experiments on single junctions in the limit of weak charging have supported the former[49] as well as the latter interpretation.[50] If $E_C/E_J>1$ and R_N is close to R_q, then the frequency of small oscillations [cf. Eq. (9)] in all single-junction models is so high that $\hbar\omega_J>2\Delta$. In this case it is plausible that a sufficient fraction of relevant frequency modes samples the region above twice the gap and the effective damping resistance R should be the normal-state resistance R_N.[40] In arrays, on the other hand, the characteristic frequency would be the spin-wave frequency which depends on the lattice constant and tends to zero for long wavelengths.

In models based on the AES effective action the damping is due to quasiparticle excitations, and is parametrized in terms of the microscopically defined matrix element $\langle|T|^2\rangle\sim 1/R_N$. These models differ from those based on the CL action in two other respects: charge transfer is explicitly discrete and not continuous as modeled in the case of an Ohmic shunt, and the highly nonlinear quasiparticle conductance of an ideal junction is taken into account. Physically, the nonlinear drop in conductance below the gap prevents the flow of quasiparticles across the tunnel barrier and, for a given voltage

TABLE I. The table gives the threshold values $R_{\rm crit}$ for the onset of phase coherence in models based on the Caldeira-Leggett (CL) or Ambegaokar-Eckern-Schon (AES) effective action. Values shown are $T=0$ results for single junctions and D-dimensional arrays on hypercubic lattices, $R_q\equiv h/4e^2\simeq 6.45$ kΩ. Depending on the model, dissipation is controlled by an Ohmic shunt R, the normal-state resistance R_N, or a finite subgap quasiparticle resistance $R_{\rm QP}$. The symbol * indicates that $R_{\rm crit}$ is universal only in the limit $E_C/\Delta\gg 1$.

Model	Single junction	Array	
CL (R)	R_q[a]	DR_q[b]*	
AES (R_N)	$(3/4)^{1/2}R_q$[c]*	$(3/16)^{1/2}DR_q$[c]*	
		$0.74R_q$	$D=2$[d]*
AES ($R_{\rm QP}$)	$(2/\pi^2)R_q$[e]*	$0.62R_q$	$D=1$
		$1.2R_q$	$D=2$[f]*
		$1.7R_q$	$D=3$

[a]References 34–39.
[b]References 42, 43, and 45.
[c]Reference 41.
[d]References 46 and 51.
[e]Reference 52.
[f]Reference 53.

$V=Q/C$, allows for some additional accumulation of charge Q.[33] Thus for energies below the gap the quasiparticle damping leads to an increase in the effective capacitance to $C'=C+\delta C$ and the AES action corresponds to the Hamiltonian, Eq. (8), with C replaced by C'. Explicit calculation gives[13,33]

$$\delta C=\tfrac{3}{16}(R_q/R_N)(e^2/\Delta) . \tag{11}$$

The value of $\delta C/C$ can be quite large and even exceed unity if

$$E_C>\tfrac{8}{3}(R_N/R_q)\Delta . \tag{12}$$

In the extreme limit $C'\approx\delta C$ the effective charging energy becomes independent of geometrical capacitance C and the Anderson-Abeles condition Eq. (7) gives a universal threshold for phase coherence.[41] However, Eq. (9) implies characteristic frequencies $\hbar\omega_J>2\Delta$. Thus capacitance renormalization might not be applicable for single junctions in this limit as the frequencies are too high to sample nonlinearities due to the gap. On the other hand, because of the lower spin-wave frequencies this problem might not be as critical in arrays.

For two-dimensional arrays at $T=0$ initial calculations[46,47] found a weak, logarithmic dependence of $R_{\rm crit}$ on E_C/Δ, giving a nonuniversal threshold. Still, for reasonable values $E_C/\Delta\cong 0.01-0.1$ the threshold value does not deviate by more than 30% from R_q. The data are more consistent with a more detailed version[51] of the work in Ref. 46 which leads to a value of $R_{\rm crit}$ independent of E_c/Δ in the limit $E_c/\Delta\gg 1$.

In addition, there are models[52,53] which take the nonideal nature of actual junctions into account by incorporating a finite, linear subgap resistance $R_{\rm QP}$ into the AES formalism. In these models the threshold is controlled by the condition $R_{\rm QP}<R_{\rm crit}$ and the boundary between phase-coherent and -incoherent states as a function of E_C/E_J is qualitatively very similar to the CL models discussed above.

C. Effect of disorder

In an ordered square array of identical junctions the overall array resistance is equal to the resistance of a single junction. In any actual thin film the individual junction resistances as well as capacitances vary according to some distribution because of the randomness in grain or cluster sizes and spacings. It is therefore necessary to incorporate the effects of disorder in the models.

We may consider the various levels at which percolation is important in ultrathin films of superconducting material: at the level of metallic connectedness, at the level of the network of normal (single-electron) tunneling paths, and at the level of Josephson-coupled tunneling paths. In the following it will be assumed that the metal coverage p is below the metallic percolation threshold p_c and that the film resistance is dominated by the resistance of the tunneling paths between clusters.

Particularly in the early stages of film growth not all junctions will be Josephson-like. Thus the corresponding bond percolation must be described by a fraction p_J of Josephson junctions. Within connected clusters of Josephson junctions the existence of phase coherence is then determined by temperature and the strength of phase fluctuations. Any nonsuperconductive bonds between cluster which are in the current path will dominate the resistance at low temperatures $T<T_c$. Of course, once the Josephson bonds have percolated across the lattice, i.e., $p_J\geq p_{Jc}$ [$=\frac{1}{2}$ for two-dimensional (2D) bond percolation], single-particle bonds are effectively shorted out. By making p_J a function of sample parameters like tunnel distance s and temperature, percolation models are able to reproduce evolutions from insulating to quasireentrant to superconducting behavior.[28,54,55]

The temperature dependence of p_J in standard models enters by assuming the condition Eq. (6). A numerical simulation by Orr *et al.*[8,54] on a square lattice with random bond strengths shows that even under the simplifying assumption $E_C=0$ insulating as well as quasireentrant and fully superconducting behavior can be reproduced as functions of p_J and R_N. Since this type of model relies on a knowledge of p_J and, in general, E_C, which are actually not known for disordered films, quantitative comparison with experiment is not possible.

Once $p_J>p_{Jc}$ the Josephson junction bonds span the whole lattice and all of the remaining $1-p_J$ single-particle junctions can be neglected at low enough temperatures. In this case the subsystem of Josephson bonds can be considered an array and treated within the theoretical framework of the ordered array models discussed above in order to find the onset of phase coherence, provided the effects of disorder are negligible.

The main effect of disorder is to establish a distribution of junction resistances. This is because charge transport is assumed to occur by tunneling, and any variation in cluster spacings leads to an exponential variation in the tunnel resistance,[56] but only to a linear variation in the corresponding charging energy. It is therefore reasonable to assume an average value for E_C throughout the array. This approximation is also justified *a posteriori* in that the threshold models as discussed above show a logarithmic dependence on E_C, if any at all.

In order to relate the distribution of junction resistances to the overall measured resistance, we map the junctions onto bonds in a completely filled regular lattice where neighboring sites correspond to neighboring clusters. The conductance of the ith bond is g_i. There are several ways to calculate the effective resistance of the resulting resistor network.[57] Within the effective medium approximation it can be shown that, for any smooth and sufficiently broad distribution of conductances $f(g_i)$, the overall network resistance is given by the resistance of the $(1-p_c)$th percentile of $f(g_i)$.[57] For the case important here, namely two-dimensional bond percolation where $p_c=\frac{1}{2}$ on a square lattice, the problem therefore is reduced to relating the overall measured resistance to the median of the distribution of the individual resistances.

The same conclusion was also reached by Ambegaokar, Halperin, and Langer[58] on the basis of a geometrical argument. In fact, it can be shown that the conjecture by Ambegaokar *et al.* is exact for any smooth distribution

on a square lattice.[59] Computer simulations provide strong evidence[60] that the conjecture is quantitatively accurate for bond as well as site percolation in two dimensions.

The above discussion can now be applied to the problem of the threshold for superconductivity.[61] If there is a single-junction threshold at a resistance R equal to $R_{\rm crit}$, then for all junctions with resistances much greater than $R_{\rm crit}$ the phase fluctuations are not quenched and the junctions consequently are not phase locked and are resistive. Junctions with resistances much less than $R_{\rm crit}$ are completely phase locked and the corresponding clusters are very strongly coupled, essentially forming one larger superconducting cluster. For the purpose of finding the threshold for phase locking the former set of junctions can therefore be taken out and the latter replaced with superconducting wires. We are then left with a subset of junctions with resistances the order of $R_{\rm crit}$. This subset percolates across the film when the measured overall film resistance equals $R_{\rm crit}$. This is because the measured resistance in two dimensions for any smooth distribution corresponds to the $(1-p_c)$th percentile of that distribution which is also the bond percolation threshold since $p_{Jc}=\frac{1}{2}$ (i.e., $1-p_c=p_c$ when $p_c=\frac{1}{2}$). Only this subset is important for the threshold. Its members cover only a narrow slice of the original broad distribution of junction resistances. Thus the disordered array has been renormalized into a weakly disordered system. On the basis of this argument the threshold results derived from calculations on ordered arrays are expected[42,43] to be relatively insensitive to the introduction of disorder into the array. The same conclusion can also be reached in the limit $E_C/\Delta \gg 1$ by explicitly considering the effect of disorder on the effective action.[45] In the extreme case that the critical subset consists only of very few members, a reduction of the problem to a single-junction threshold might be appropriate.[40,43]

V. DISCUSSION

Comparing the observed $T_c^{\rm loc}$ versus R_N data (Fig. 3) with the predictions of localization theory for microscopically disordered systems we find a much weaker dependence on R_N than expected theoretically.[18] If R_N indeed were produced by microscopic disorder, then over the interval shown in the figure the theories would predict a complete depression of T_c. From Fig. 2 we see that in all systems studied, even at the very early stages of film evolution, the signature of superconductivity in the form of a kink or a dip in the $R(T)$ curves appears at temperatures fairly close to the transition temperature of thicker films in the same sequence. We interpret these results as an indication of the percolative nature of the films, where R_N is dominated by the intercluster and not the intracluster resistance. This means that the local transition is determined by clean, metallic clusters with small, bulklike internal resistivity ρ_0. The absence of microscopic disorder due to impurities is not surprising considering the ultrahigh-vacuum conditions of less than 2×10^{-10} torr background pressure during evaporations.

From the criterion given by Eq. (1) for the onset of local superconducting order the grain sizes L in the films must be in excess of $L_{\rm crit}$, because for grains of sizes close to $L_{\rm crit}$ fluctuations in the order parameter would wipe out any transition.[24] Such fluctuations might, on the other hand, be the source of the weak logarithmic T_c depression that we observe in Ga, which is although significant not sufficient to destroy local superconductivity. The nominal thicknesses of the Ga films were approximately a factor 3 smaller than the Pb, Al, and In films over the same range in the evolution of $R(T)$. It is also conceivable that in such films, which are the equivalent of only about three monolayers in nominal thickness, boundary effects or peculiarities of the growth mechanism might affect $T_c^{\rm loc}$. Nevertheless the observed weak depression does not change the general conclusion of a cluster size $L \gg L_{\rm crit} \simeq 30$ Å which is therefore also much larger than the film thickness d.

The films do not exhibit a pronounced two-stage resistive transition, where the drops in $R(T)$ on the local and global level are separated by a small temperature interval over which there is some intermediate resistance. Such clearly separated transitions have been observed in certain granular systems with also much lower overall sheet resistance such that the intragrain resistance is an appreciable fraction of the intergrain barrier resistance. Examples of this behavior have been found in Al-Ge films, Hg-Xe films, as well as in microlithographically fabricated Josephson junction arrays.[62]

The data in Fig. 2 clearly show that as a film grows in thickness, superconducting order is established on grains or clusters of grains before superconducting coupling develops between them. The critical current $I_c=(2e/\hbar)E_J$ for pair tunneling evidently is suppressed in these very highly resistive films and activated quasiparticle tunneling is the dominant process. This changes once the dip in the $R(T)$ traces develops later in the evolution, signaling that a significant fraction of the junctions possess a finite I_c and are phase locked.

An important question which might be asked is at which point in the film evolution do Josephson junctions span the sample. This can perhaps be determined from the shape of the I-V characteristics, although at present there is no theory available for quantitative comparison. From Fig. 4 we see that quasi-particle-like I-V characteristics persist in the film evolution until the quasireentrant $R(T)$ traces give way to traces characterized by flat tails at low temperatures. It can be argued that at this point Josephson junctions must have percolated across the film because the subsequent I-V traces in the evolution show Josephson-like nonlinear behavior at high currents. This, however, leaves open the question if the observed pronounced quasireentrance before this point is due to the fact that $p_J < p_{Jc}$ or is due to collective effects. Furthermore, any reentrance predicted by quantum X-Y models without dissipation[31] as well as by models incorporating dissipation within the CL (Refs. 35–38, 43, and 44) and AES (Ref. 53) formalisms, depends sensitively on E_C. Without an independent determination of E_C a quantitative comparison with experiment is not possible.

Turning now to the onset of global superconductivity, the data of Figs. 5–7 show that the onset of a zero-resistance state across the whole film at low temperatures is determined by the normal-state sheet resistance. Other factors like total nominal film thickness or material parameters (crystalline or amorphous microstructure, strong or weak coupling) do not appear to be relevant. There are several questions connected with this observed resistance threshold, namely the precise value of $R_{\rm crit}$, its universality, and the nature of the critical region $R_N \geq R_{\rm crit}$ as the zero-resistance state is approached from above.

The existence of a sheet resistance controlled threshold for global phase coherence is incompatible with a control parameter of form $E_J/E_C=(R_q/R_N)(C\Delta/e^2)$ as in the Anderson-Abeles condition Eq. (7). Even in the extremely unlikely case that the thickness variation shown in Fig. 6 did not change C at all, variations in Δ should have had a significant effect on the threshold since the ratios $\Delta_{\rm Ga}:\Delta_{\rm Pb}:\Delta_{\rm Sn}:\Delta_{\rm Al}=8.4:7.2:3.1:1$ if bulk values are used.

In both the CL and AES formalisms there is, at least in the limit of strong charging $E_C/\Delta>1$ and at $T=0$, a universal threshold for the onset of phase coherence. In this limit phase coherence is controlled solely by the effective damping resistance (R, R_N, or $R_{\rm QP}$) and the threshold is connected with a particular, universal value $R_{\rm crit}$ as given in Table I. The theoretical value for $R_{\rm crit}$ might be expected to vary considerably depending on the model assumptions and particularly due to collective effects in arrays. To some degree this is confirmed by a comparison of the models. Still, all zero-temperature results for arrays in two dimensions and large E_C/Δ are close (within a factor 2 or less) to $R_{\rm crit}=R_q\simeq 6.45\ {\rm k}\Omega/\Box$. The single-junction results in general differ from the array values by not more than one would expect from the difference in coordination numbers. In fact, the main difference between the threshold values for different dimensions D is simply the difference in coordination numbers $z=2D$. Threshold results for ordered arrays might be relatively insensitive to disorder as argued in the previous section, but in the limit of extremely strong disorder one-dimensional chains or even single junctions could dominate the whole array. Such changes in the effective coordination number would tend to move $R_{\rm crit}$ to lower values. All array models based on the CL or AES effective actions (with the exception of the model of Ref. 43) have used a self-charging approximation for the capacitance tensor, i.e., ignored off-diagonal elements. There is some indication that this does not produce qualitative changes.[53] For a quantitative comparison with experiment it might, however, be important to consider the full form of the tensor. Therefore all that the present theoretical models can say is that the zero-temperature threshold value $R_{\rm crit}$ is close to R_q, probably within a factor of 2 as long as E_C/Δ is large enough.

The relevant charging energy entering into the Hamiltonian in all models is the bare (or geometrical) charging energy E_C, i.e., neglecting any effective renormalization of the capacitance C due to the coupling of grains by tunneling.[26] Although we were not able to determine the geometrical capacitance *in situ*, we can estimate E_C. As discussed above, the typical cluster size L is presumably much larger than 30 Å. This leads to $C\gg 3\times 10^{-18}$ F, or $E_C\ll 160$ K, if an effective dielectric constant $\epsilon\sim 10$ is assumed. A lower bound on E_C might be obtained from the $R(T)$ characteristics in the normal state. The data in the early stages of film growth in Figs. 2(a)–2(d) are best fit to $R(T)\sim\exp(A/T)$. We assume that the normal-state activation A energy measured in the thinnest films is a representative lower bound for the unrenormalized E_C and that the latter does not change substantially as R_N approaches R_q. The observed activation energies of up to 20–30 K imply $C\ll 3\times 10^{-17}$ or $L<300$ Å for $\epsilon\sim 10$. The considerations also imply $E_C/\Delta>1$.

The experimental finding that R_N controls the onset of phase coherence seems to exclude the models of Refs. 52 and 53 unless $R_{\rm QP}=R_{\rm QP}(R_N)$. It also suggests the identification $R=R_N$ is necessary in models based on the CL action.

Experimentally the value of $R_{\rm crit}$ is bracketed by the data in Fig. 6 to within about 25%. The data in Fig. 6 also depended on the somewhat arbitrary definition of zero resistance by the limit of experimental resolution. A much more useful way to determine $R_{\rm crit}$ therefore is the one shown in Fig. 7. Because this approach required a high density of data points in the region $R_N\simeq R_{\rm crit}$, only the four sequences of films shown could be used. The solid lines are guides to the eye. If they are extrapolated to lower $R(0.7\ {\rm K})$, they asymptotically approach a critical resistance $R_{\rm crit}\sim R_q$.

Experimental uncertainties enter in the determination of $R(0.7\ {\rm K})$ and $R(14.0\ {\rm K})\equiv R_N$. Another factor is the error in the determination of the width and length of the film segment between the voltage probes in order to obtain the correct conversion to sheet resistance. We estimate this error to be less than 10%. Uncertainties in the values of $R(0.7\ {\rm K})$ stem from voltage resolution while measuring resistance in the flat-tail regions (see Fig. 8). Higher values for the excitation currents would increase the resistance resolution, but the values were chosen to safely avoid nonlinear or heating effects. However, the uncertainty in determining $R_{\rm crit}$ is rather small as determined from Fig. 7 because of the exponential dependence of $R(0.7\ {\rm K})$ on R_N below $10\ {\rm k}\Omega/\Box$. For the same reason the Al data in Fig. 7 are representative, even though in that case at the lowest attainable temperature, 0.6 K, the flattening off of the $R(T)$ was not as fully developed as in the case of Ga and Pb. In defining a sensible normal-state film resistance, the small, but in most sequences significant, negative temperature coefficient of resistance (TCR) has to be taken into account. We assume that the correct choice is the resistance in the normal state at a temperature of order Δ/k [and not, e.g., $R(300\ {\rm K})$]. Since we observed a TCR less than $0.1\ k\Omega/{\rm K}$ [cf. Figs. 2 and 5(b)] below $R_N=10\ {\rm k}\Omega/\Box$, we believe that the operational definition $R_N\equiv R(14\ {\rm K})$ provides a good estimate of the correct normal-state resistance. Taken together, the experimental uncertainties lead to an overall accuracy of 15% or better in the determination of the threshold

value R_{crit} for global superconductivity.

A threshold value $R_{crit} \simeq R_q$ is also compatible with the data available from other workers. Data by Imry and Strongin[21] and Hebard and Paalanen[63] in addition show a significant depression of T_c^{loc} from the bulk values T_c, most likely due to disorder on a microscopic scale. The data by Dynes *et al.*[15] and White *et al.*,[16] on the other hand, exhibit local transition temperatures fairly close to the bulk values as expected in cleaner granular films. Studies of random arrays of oxidized granular Sn particles are also consistent with a threshold at $R_N = R_q$.[64]

In three-dimensional granular films the relevant parameter is the resistivity ρ and not the sheet resistance R. But we can assume $\rho_{crit} = R_{crit} L$, where L is an appropriate length. Estimating L from the effective superconducting cluster size (determined from critical fields) data on three-dimensional granular Al (Ref. 65) films appear to obey the threshold $R_{crit} = R_q$.

Recent measurements[66] on microfabricated regular two-dimensional arrays of small aluminum tunnel junctions show a striking resemblance to the data in Figs. 2(a)–2(d). Global phase coherence was found only in arrays with $R_N \leq 5$ kΩ/□, a value somewhat below our results on ultrathin films but still in good agreement with array models in the limit $E_C/E_J \gg 1$ (see Table I). Since E_C/E_J is only of order unity in these arrays, this might imply universality over a larger range E_C/E_J than predicted by the available models for $D=2$. In addition, data on single Sn-SnO_x-Sn tunnel junctions[67] in the same regime $E_C/E_J \geq 1$ indicate a transition to a resistive low-temperature state as R_N exceeds R_q.

A final point concerns not so much the value of the threshold but rather the way it is approached as $R_N \to R_q$ (Fig. 7). A detailed calculation of the functional dependence of $R(0.7\text{ K})$ on $R(14.0\text{ K})$ is lacking at present. However, it is tempting to interpret the data in Fig. 7 as critical region above a resistance-controlled phase transition at R_q.[68,69] In such case zero-point phase fluctuations play the role of an effective temperature $T_{eff} \propto E_C$ (Ref. 30) and the flux-flow resistance just above the transition of the resulting quantum X-Y model might be described by the corresponding classical flux-flow model[32] if the control parameter T/T_{KT} is replaced by T_{eff}/T_{crit}. Dissipation will reduce the zero-point fluctuations and thereby T_{eff}, which, given Eqs. (11) and (12), is proportional to R_N. Based on this argument we might expect the low-temperature resistance to vary as

$$R(T \to 0) = A \exp[-B(R_N/R_{crit} - 1)^{1/2}] , \qquad (13)$$

where A and B are constants. Figure 9 shows the agreement of the Ga and Pb data with this heuristic model. Independent fits to Eq. (13) for all three data sets give a value $R_{crit} = 6.5$ kΩ/□ to within 2%, supporting the idea of a universal threshold value at or close to $R_q = h/(2e)^2$. For the Al data, on the other hand, we only obtained a comparatively poor fit to Eq. (13), which might have been influenced by the fact that we were unable to obtain resistance data at low enough temperatures, i.e., far enough into the flat-tail region.

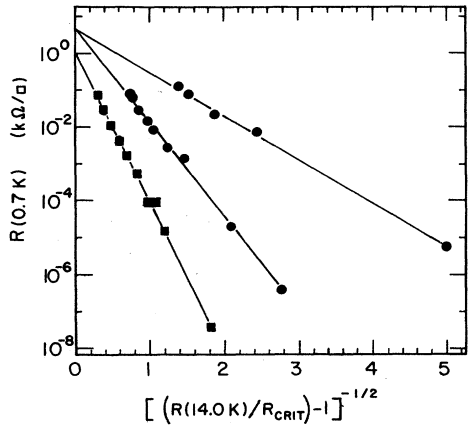

FIG. 9. Plotted is the resistance of the flat tail, $R(0.7\text{ K})$, vs a function of the normal-state resistance. This plot is motivated by the Halperin-Nelson formula where the temperature is replaced by the resistance as the control parameter for a transition to superconductivity. Data for Pb (■) and Ga (●) films find the best fit with R_{crit} adjusted to $R_{crit} = R_q$.

VI. CONCLUSION

The available experimental data suggest a threshold for global phase coherence at or very close to $R_q \equiv h/4e^2 \simeq 6.45$ kΩ/□ independent of any other material parameters. Such a threshold is incompatible with traditional criteria based on the classical or quantum X-Y models. It is explained by theoretical models that include coupling of the macroscopic phase variable to dissipation or contain capacitance renormalization. While the data support the notion of a universal value for the threshold, from the theory available at present it is not clear that the universality at $T=0$ survives at finite temperatures.

If the threshold indeed is nonuniversal because the boundary between the phase-coherent and phase-incoherent state exhibits a dependence on the ratio Δ/E_C, then in principle this could be tested experimentally. For our Ga and Pb sequences the gaps were rather similar, but the nominal total thicknesses at the threshold varied by a factor of about 3. If we guess that this changed the charging energy by roughly the same factor, the sensitivity to the ratio Δ/E_C would have led to a noticeable change in R_{crit} if the available calculations are representative. The same argument applies to Sn and Ga where the gaps Δ are different by a factor of 3. Clearly, a stronger test was achieved by using a material with even smaller gap such as Al. There are several outstanding problems which remain. There is considerable uncertainty as to the precise connection between the shunting resistance in the junction lattice models, and the normal-state sheet resistance of the films. Because the resistance is a coupling parameter in all of the models it should never be universal, a fact which appears to be in conflict with the weight of the experimental evidence supporting universality, but which is not yet established definitely.

Another, possibly more fundamental difficulty with the theory, is the fact that in the microscopic derivation of the effective Hamiltonian, charging energies are ignored at the outset. Degenerate perturbation theory is used and only later are charging correlations included as an independent term. In the presence of strong charging effects, as in the case of all of the relevant models, this treatment might not be correct, requiring charging corrections to be taken into account at the outset of the derivation of the effective Hamiltonian.[70]

The outstanding experimental question at this point is whether the threshold is precisely universal, and to what extent the strong charging limit is required. The outcome of experiments studying the onset of superconductivity in films which are continuous rather than composed of metal islands may resolve the issue. In such systems the transition temperature is substantially depressed in the thinnest films. If there were nevertheless a universal threshold for zero resistance at low temperatures dependent on normal-state resistance, then arguments more general than the ones presented thus far would be needed to explain the onset.[71]

ACKNOWLEDGMENTS

The authors would like to thank the personnel of the machine shop at the University of Minnesota for their invaluable assistance in building and maintaining the equipment. A number of individuals contributed substantially to our understanding of this problem. They include V. Ambegaokar, S. Chakravarty, S. Doniach, R. C. Dynes, R. A. Ferrell, M. P. A. Fisher, B. Halperin, S. Kivelson, A. J. Leggett, B. Mirhashem, T. V. Ramakrishnan, A. Schmid, G. Schön, and G. Zimanyi. We would in addition like to especially thank C. G. Kuper for his very important assistance at the early stages of this work. We are indebted to the late James Michael Gordon for his encouragement. This work was supported by the Low Temperature Physics Program of the National Science Foundation under Grant No. NSF/DMR-85-03087.

---

*Present address: Center for Submicron Technology, P.O. Box 5046, 2600, GA, Delft, The Netherlands.

†Present address: Department of Physics, University of Michigan, Ann Arbor, MI 48109.

[1]A. I. Shal'nikov, Zh. Eksp. Teor. Fiz. **10**, 630 (1940); Nature, **142**, 74 (1938).

[2]W. Buckel and R. Hilsch, Z. Phys. **138**, 109 (1954); W. Buckel, *ibid.* **138**, 136 (1954).

[3]Gerd Bergmann, Phys. Rep. **27**, 159 (1976).

[4]R. E. Glover, Phys. Lett. **25A**, 542 (1967); for a review see W. J. Skocpol and M. Tinkham, Rep. Prog. Phys. **38**, 1049 (1975).

[5]Gerd Bergmann, Phys. Rep. **107**, 1 (1984).

[6]For a collection of articles see *Localization, Interaction and Transport Phenomena,* edited by B. Kramer, G. Bergmann, and Y. Bruynseraede (Springer-Verlag, Berlin, 1985).

[7]B. G. Orr, H. M. Jaeger, and A. M. Goldman, Phys. Rev. Lett. **53**, 2046 (1984).

[8]B. G. Orr, H. M. Jaeger, and A. M. Goldman, Phys. Rev. B **32**, 7586 (1985); an alternative analysis of the local minimum has been given in D. E. Haviland, H. M. Jaeger, D. G. Orr, and A. M. Goldman, Phys. Rev. B (to be published).

[9]B. G. Orr, H. M. Jaeger, A. M. Goldman, and C. G. Kuper, Phys. Rev. Lett. **56**, 378 (1986).

[10]H. M. Jaeger, D. B. Haviland, A. M. Goldman, and B. G. Orr, Phys. Rev. B **34**, 4920 (1986).

[12]A. O. Caldeira and A. J. Leggett, Phys. Rev. Lett. **46**, 211 (1981); Ann. Phys. (N.Y.) **149**, 373; **153**, 445(E) (1984).

[13]V. Ambegaokar, U. Eckern, and G. Schon, Phys. Rev. Lett. **48**, 1745 (1982).

[14]B. Abeles, Phys. Rev. B **15**, 2828 (1977); P. W. Anderson, in *Lectures on the Many Body Problem,* edited by E. R. Caianello (Academic, New York, 1964), Vol. 2, p. 127.

[15]R. C. Dynes, J. P. Garno, and J. M. Rowell, Phys. Rev. Lett. **40**, 479 (1978).

[16]A. E. White, R. C. Dynes, and J. P. Garno, Phys. Rev. B **33**, 3549 (1986).

[17]D. G. Naugle, R. E. Glover III, and W. Moormann, Physica **55**, 250 (1971).

[18]H. Ebisawa, H. Fukuyama, and S. Maekawa, J. Phys. Soc. Jpn. **54**, 2257 (1985).

[19]J. M. Graybeal and M. R. Beasley, Phys. Rev. B **29**, 4167 (1984); S. I. Park and T. H. Geballe (1985), Physica B+C **135B**, 108 (1985).

[20]G. Deutscher, Y. Imry, and L. Gunther, Phys. Rev. B **10**, 4598 (1974).

[21]Y. Imry and M. Strongin, Phys. Rev. B **24**, 6353 (1981).

[22]M. Strongin, R. S. Thompson, O. F. Kammerer, and J. E. Crow, Phys. Rev. B **1**, 1078 (1970).

[23]P. W. Anderson, J. Phys. Chem. Solids **11**, 26 (1959).

[24]B. Mühlschlegel, D. J. Scalapino, and R. Denton, Phys. Rev. B **6**, 1767 (1972).

[25]V. Ambegaokar and A. Baratoff, Phys. Rev. Lett. **10**, 486 (1963).

[26]E. Ben-Jacob, E. Mottola, and G. Schön, Phys. Rev. Lett. **51**, 2064 (1983); R. Brown and E. Šimańek, Phys. Rev. B **34**, 2957 (1986).

[27]M. Tinkham, *Introduction to Superconductivity* (McGraw-Hill, New York, 1975).

[28]G. Deutscher, O. Entin-Wohlman, S. Fishman, and Y. Shapiro, Phys. Rev. B **21**, 5041 (1980); O. Entin-Wohlman, A. Kapitulnik, and Y. Shapiro, *ibid.* **24**, 6464 (1981)

[29]V. L. Berezinskii, Zh. Eksp. Teor. Fiz. **59**, 907 (1970) [Sov. Phys.—JETP **34**, 610 (1971)]; J. M. Kosterlitz and D. J. Thouless, J. Phys. C **6**, 1181 (1973).

[30]W. L. McLean and M. T. Stephen, Phys. Rev. B **19**, 5925 (1979); S. Doniach, *ibid.* **24**, 5063 (1981); E. Šimańek, Phys. Lett. **101A**, 161 (1984); L. Jacobs, J. V. José, M. A. Novotny, and A. M. Goldman, Europhys. Lett. **3**, 1295 (1987).

[31]S. Doniach, in *Percolation, Localization, Superconductivity,* Vol. 109 of *NATO Advanced Study Institute, Series B: Physics,* edited by A. M. Goldman and S. A. Wolf (Plenum, New York, 1984), p. 401; K. B. Efetov, Zh. Eksp. Teor. Fiz. **78**, 2017 (1980) [Sov. Phys.—JETP **51**, 1015 (1980)]; P. Fazekas, B. Mühlschlegel, and M. Schroter, Z. Phys. B **57**, 193 (1984); R. S. Fishman and D. Stroud, Phys. Rev. B **37**, 1499 (1988); L. Jacobs, J. V. José, and M. A. Novotny, Phys. Rev. Lett. **53**,

2177 (1984); J. V. José, Phys. Rev. B **29**, 2836 (1984); S. Maekawa, H. Fukuyama, and S. Kobayashi, Solid State Commun. **37**, 45 (1980); E. Šimańek, *ibid.* **31**, 419 (1979); Phys. Rev. B **23**, 5762 (1982); **32**, 500 (1985).

[32]A. M. Kadin, K. Epstein, and A. M. Goldman, Phys. Rev. B **26**, 3950 (1982).

[33]V. Ambegaokar, in *Percolation, Localization, and Superconductivity,* Vol. 109 of *NATO Advanced Study Institute, Series B: Physics,* edited by A. M. Goldman and S. A. Wolf (Plenum, New York, 1984), p. 43; U. Eckern, G. Schön, and V. Ambegaokar, Phys. Rev. B **30**, 6419 (1984).

[34]A. Schmid, J. Low Temp. Phys. **49**, 609 (1982); Phys. Rev. Lett. **51**, 1506 (1983).

[35]M. P. A. Fisher and W. Zwerger, Phys. Rev. B **32**, 6190 (1985); C. Aslangul, N. Pottier, and D. Saint-James, J. Phys. (Paris) **48**, 1093 (1987).

[36]M. P. A. Fisher, Phys. Rev. Lett. **57**, 885 (1986).

[37]U. Eckern and F. Pelzer, Europhys. Lett. **3**, 131 (1986).

[38]W. Zwerger, Phys. Rev. B **35**, 4737 (1987).

[39]A. D. Zaikin and S. V. Panyukov, Phys. Lett. A **120**, 306 (1987).

[40]B. G. Orr, J. R. Clem, H. M. Jaeger, and A. M. Goldman, Phys. Rev. B **34**, 3491 (1986); M. Fibich, C. G. Kuper, M. Revzen, and Amiram Ron, J. Low. Temp. Phys. **69**, 459 (1987).

[41]R. A. Ferrell and B. Mirhashem, Phys. Rev. B **37**, 648 (1988); Physica C **152**, 361 (1988).

[42]S. Chakravarty, G.-L. Ingold, S. Kivelson, and A. Luther, Phys. Rev. Lett. **56**, 2303 (1986).

[43]M. P. A. Fisher, Phys. Rev. B **36**, 1917 (1987).

[44]E. Šimańek and R. Brown, Phys. Rev. B **34**, 3495 (1986).

[45]S. V. Panyukov and A. D. Zaikin, Phys. Lett. A **124**, 325 (1987).

[46]S. Chakravarty, S. Kivelson, G. Zimanyi, and B. I. Halperin, Phys. Rev. B **35**, 7256 (1987).

[47]S. V. Panyukov and A. D. Zaikin, Jpn. J. Appl. Phys. Suppl. **26-3**, 1327 (1987).

[48]A. Barone and G. Paterno, *Physics and Applications of the Josephson Effect* (Wiley, New York, 1982).

[49]L. D. Jackel, J. P. Gordon, E. L. Hu, R. E. Howard, L. A. Fetter, D. M. Tennant, R. N. Epworth, and J. Kurkijarvi, Phys. Rev. Lett. **47**, 697 (1981); P. Silvestrini, S. Pagano, R. Christiano, O. Liengme, and K. E. Gray, *ibid.* **60**, 844 (1988).

[50]S. Washburn, R. A. Webb, R. F. Voss, and S. M. Farris, Phys. Rev. Lett. **54**, 2712 (1985).

[51]S. Chakravarty (private communication).

[52]F. Guinea and G. Schön, Euophys. Lett. **1**, 585 (1986).

[53]A. Kampf and G. Schön, Phys. Rev. B **36**, 3651 (1987); Physica B+C **152B**, 239 (1988).

[54]B. G. Orr, Doctoral dissertation, University of Minnesota, Minneapolis, 1985 (unpublished).

[55]E. Šimańek, Phys. Rev. B **25**, 237 (1982).

[56]C. G. Neugebauer and M. B. Webb, J. Appl. Phys. **33**, 74 (1962).

[57]S. Kirkpatrick, in *Ill-Condensed Matter,* edited by R. Balin, R. Maynard, and G. Toulouse (North-Holland, New York, 1979), p. 321.

[58]V. Ambegaokar, B. I. Halperin, and J. S. Langer, Phys. Rev. B **4**, 2612 (1971).

[59]B. I. Halperin (private communication).

[60]D. Berman, B. G. Orr, H. M. Jaeger, and A. M. Goldman, Phys. Rev. B **33**, 4301 (1986).

[61]H. M. Jaeger, Doctoral dissertation, University of Minnesota, Minneapolis, 1987 (unpublished).

[62]G. Deutscher and M. L. Rappaport, J. Phys. (Paris) Colloq. **6**, C6-581 (1978); K. A. Epstein, A. M. Goldman, E. D. Dahlberg, and R. Mikkelson, in *Inhomogeneous Superconductors—1979 (Berkeley Springs, WV),* Proceedings of the Conference on Inhomogeneous Superconductors, AIP Conf. Proc. No. 58, edited by D. U. Gubser, T. L. Francavilla, S. A. Wolf, and J. R. Leibowitz (AIP, New York, 1979), p. 58; J. M. Gordon and A. M. Goldman, Phys. Rev. B **30**, 4063 (1984).

[63]A. F. Hebard and M. A. Paalanen, Phys. Rev. B **30**, 4063 (1984).

[64]M. Kunchur, P. Lindenfeld, W. L. McLean, and J. S. Brooks, Phys. Rev. Lett. **59**, 1232 (1987); M. Kunchur, Y. Z. Zhang, P. Lindenfeld, W. L. McLean, and J. S. Brooks, Phys. Rev. B **36**, 4062 (1987).

[65]S. Kobayashi, Physica B+C **152B**, 223 (1988).

[66]L. J. Gerligs and J. E. Mooij, Physica B+C **152B**, 212 (1988).

[67]M. Iansiti, A. T. Johnson, Walter F. Smith, H. Rogalla, C. J. Lobb, and M. Tinkham, Phys. Rev. Lett. **59**, 489 (1987).

[68]H. M. Jaeger, D. B. Haviland, A. M. Goldman, and B. G. Orr, in *Weak Superconductivity,* edited by A. Barone and A. Larkin (World Scientific, Singapore, 1987), p. 96; Physica B+C **152B**, 218 (1988).

[69]W. Zwerger, Physica B+C **152B**, 236 (1988).

[70]E. Shimshoni, Y. Geffen, and S. Fishman, Phys. Rev. B (to be published).

[71]Studies of continuous films suggest a somewhat different type of threshold than the one discussed here for granulated films. See, D. B. Haviland, Y. Liu, and A. M. Goldman, Phys. Rev. Lett. **62**, 2180 (1989).